Efficient V2X Waveforms: NOMA combined with FBMC/UFMC reduces the Co-channel Interference

Rafik Zitouni, Francesco Corrado Casto, Sebti Mouelhi, Benaoumeur Senouci

Efficient V2X Wavefroms: NOMA combined with FBMC/UFMC reduces the Co-channel Interference

Rafik Zitouni[†], Francesco Corrado Casto[‡], Sebti Mouelhi[⋆] and Benaoumeur Senouci[◇]
5G/6GIC, Institute for Communication Systems, University of Surrey, U.K. [†]
Department of Electronics and Telecommunications, Politecnico di Torino, Torino, Italy[‡]
ESTACA École d'ingénieurs, Groupe ISAE, Montigny-le-Bretonneux, France[⋆]
ECE Department, North Dakota State University, USA / CIM, Southern Denmark University, Denmark[◇]
Email: r.zitouni@surrey.ac.uk, francescocorrado.casto@studenti.polito.it, sebti.mouelhi@estaca.fr, senouci@sdu.dk

***Abstract*—IEEE 802.11p/bd and 3GPP LTE-Vehicular & 5G NR-V2X technologies counteract the doubly-selectivity properties of wireless vehicular communications thanks to the Orthogonal Frequency Division Multiplexing (OFDM). However, this waveform is the source of adjacent channel interference caused by high out-of-band emissions and luck of spectrum access fairness as well as channel capacity limitations. Filter Bank Multiple Carrier (FBMC) and Universal Filtered Multiple Carrier (UFMC) are efficient waveforms reducing the inter-channel interference for 5G physical layer and beyond. This paper provides simulation measurements of the channel capacity under these waveforms by applying the Non-Orthogonal Multiple Access (NOMA) technology with respect to the 3GPP specifications. The results put in evidence less spurious emission and low Bit Error Probability (BEP) using FBMC compared to both OFDM and UFMC waveforms. The spectral efficiency is enhanced as well, thanks to the combination of NOMA with FBMC. The simulation source code is shared for reproduction and further development.**

***Index Terms*—5G New Radio, NR-V2X, 3GPP, OFDM, NOMA, FBMC, UFMC, IEEE 802.11p/bd, Radio access technology, Vehicle-To-Everything communications (V2X).**

I. Introduction

Two main standards have been introduced to support vehicular wireless networks [1]. The first is IEEE 802.11p [2] (customized from IEEE 802.11a) and the second is the Long Term Evolution – Vehicular (LTE-V) [3], [4] (originating from 3GPP LTE cellular networks). IEEE 802.11p and LTE-V are resp. currently evolving to IEEE 802.11bd [5] and 5G NR-V2X [6], [7] (NR for New Radio). Physical and MAC layers under IEEE 802.11p handle the spontaneous Vehicular Ad-Hoc Networks (VANet) where messages are peer-to-peer rooted between connected systems without base stations: the On-Board Units (OBUs) are able to directly interact one with each other and with the Road-Side Units (RSUs). Under IEEE 802.11p, the data rate is theoretically limited to 27MB/s (Megabits per second) with worst case latency up to 100ms [8]. 5G NR-V2X has been proposed as an alternative by modifying LTE-A [9] and LTE-V to support high data rate (at gigabits per second GB/s) and low latency below 1ms for V2V communications. This performance is guaranteed for sidelink communications without the intervention of a gNB (a 5G wireless base station) in data traffic for both transmission and reception.

Orthogonal Frequency Division Multiplexing (OFDM) is still the common adopted waveform for IEEE 802.11p/bd and NR-V2X. The main carrier is based on parallel and orthogonal multiple subcarriers. The Cyclic Prefix (CP) technique guarantees orthogonality, and isolates successive blocks of data symbols to prevent losses in spectral efficiency [10]. Moreover, the main carriers under OFDM could be a source of Out-Of-Band (OOB) emissions. Given that modulation is Orthogonal Multiple Access (OMA) based, the users share resources in an orthogonal way which causes congestion problems because of limited bandwidths and unfair access to the spectrum.

Other existing waveforms might overcome the mentioned issues such as Filter Bank Multiple Carrier (FBMC) [10], [11] and Universal Filtered Multiple Carrier (UFMC) [12], [13] (or filtered OFDM [14]). FBMC differs from OFDM in the choice of prototype filter at both transmitter and receiver, and exploits a CP-free model by prototyping filters resistant to doubly dispersive channels. UFMC generalizes the filtering for sub-bands decomposed into several subcarriers, whereas FBMC filters each subcarrier separately. Furthermore, Non-Orthogonal Multiple Access (NOMA) has been proposed in [15], [16], as a Radio Access Technology (RAT), to improve the capacity of channels sharing the same central frequency. It exploits power and code domain superposition in order to increase the channel capacity.

UFMC and FBMC have been already proposed for 5G NR networks as candidates but are not yet standardized. To the best of our knowledge, FBMC and UFMC combined with NOMA from the perspective of being applied to vehicular wireless networks and generally to 5G NR [17] has not been explored yet. This work falls under the standardization efforts of the 5G NR-V2X specifications. It provides a set of measurements showing how FBMC and UFMC waveforms reduce the inter-channel interference, improve the channel capacity when combined with NOMA, and distinctly demonstrate usefulness for efficient V2X communications.

The manuscript is organized as follows. Some recent related works are quoted in Section II. Section III draws an overview of NR-V2X specifications. Section IV provides details about the combination technique of NOMA with FBMC and UFMC waveforms for NR-V2X. The simulation results and details are reported in Section V. Conclusions and the work's boundaries are presented in Section VI.

II. Related work

Some related works on NOMA, FBMC and UFMC addressing their combinations challenges, merits, performance factors, applications, shortcomings, and possible standardization tracks [18] are cited in this section. In the recent work [19], the authors propose a Light Fidelity (LiFi) system combining NOMA, FBMC, and Asymmetrically-Clipped Optical (ACO). They claim that throughput could be increased by 1.8 compared to FBMC, OFDM, and OFDM-NOMA.

The authors of [20] introduce a NOMA multi-carrier waveform using UFMC modulations based on input signal phase rotation. Results show a Peak-to-Average Power Ratio (PAPR) gain of 5.4dB compared to NOMA-UFMC waveform at clip rate of 10^{-3} using 4-QAM. In [21], the authors unveil the importance of Successive Interference Cancellation (SIC) for NOMA systems, and prove that the SIC decoding order selection schemes are keys to alleviate multiple-access interference. The work [22] focuses on studying a co-existence of multiple 5G services employing OFDM and FBMC waveforms within a resilient photonic millimeter-wave mobile fronthaul architecture. They show, with the application of intra-symbol frequency-domain averaging, that the Error Vector Magnitude (EVM) performance of FBMC is comparable to that of OFDM which traditionally exhibits a better resilience to phase noise. In [23], the authors compare CP-OFDM to FBMC based on 5G waveform requirements, and studies an FBMC-derivative waveform (namely QAM-FBMC) applying multiple prototype filters and QAM modulation. It achieves the same BEP as CP-OFDM without spectrum efficiency reduction.

III. Overview of NR-V2X

As mentioned in the introduction, 5G NR-V2X upgrades LTE-V. The latter introduces a new "Mode-4" to handle V2V using PC5 sidelink interface without cellular infrastructure. NR-V2X [24], [25] is standardized with Mode 1 and Mode 2. In the first, sidelink resources are scheduled by the gNB while, in the second, a Vehicular User Equipment (V-UE) autonomously selects sidelink resources from the PC5 available pool. Evolved physical resource utilization capacities ensure quality of service in dense/highly mobile vehicular networks.

NR-V2X allows spectrum flexibility and aggregation as in classical LTE with the bandwidths 1.4MHz, 3MHz, 5MHz, 10MHz, 15MHz and 20MHz. Data rate reaches 21MB/s with 64-QAM and Discrete Fourier Transform spread OFDM (DFT-s-OFDM) carrier modulation [7] almost the same as the high level Single Carrier SC-OFDM of LTE. Radio coverage is supported up to 100km but peak performances are granted for less than 5km distances [26], [27]. However, similar to LTE-V, channels are formed by a number subcarriers divided into Resource Blocks (RBs) in frequency domain and subframes in the time domain. Every RB has a bandwidth of 180KHz wide since it is composed of 12 subcarriers of 15KHz each with a subframe of 1ms long. Two types of data are distinguished: some are for control and the others are for users resp. exchanged through Physical Sidelink Control Channel (PSCCH) and Physical Sidelink Shared Channel (PSSCH).

One of the main key issues of 5G NR sidelink is how to efficiently share the spectrum without interference while guaranteeing usage access fairness [4]. These physical resources are used in both Modes 3 and 4. It is also important to highlight the differences between sent messages types: Transport Blocks (TBs) over PSSCHs and Sidelink Control Information (SCIs) over PSCCHs. They resp. represent the transmission payload and the information messages. In order to resolve these issues, Sensing-Based Semi-Persistent Scheduling (SB-SPS) has been proposed for both modes [3], [26]. Each V-UE can transmit a random number between 5 and 15 of consecutive packets, and this number is inserted into the SCI message. This number is decremented after every single packet transmission. When zero is reached, if the previous stream has not been completed, a new random reservation is set. In addition, the time interval during which the resources are allocated is contained in the SCI message to make other V-UEs aware of the transmission delay. This algorithm causes an extra overhead by V-UE locations exchange in order to efficiently share physical resources.

OMA is the current NR-V2X RAT: the large number of V-UEs access the same spectrum resources using DFT-s-OFDM scheme. Since resources are orthogonally shared, congestion problems might occur due to the bandwidth limitations, especially when the number of V-UEs increases. These issues lead to collisions and packet loss as well. Furthermore, we can put in evidence that OFDM waveforms produce spurious emissions causing the phenomenon of Adjacent Channel Interference (ACI) [28]. In view of these facts, implementing new waveforms and RATs would improve not only 5G NR-V2X, but also performances of cellular networks in general.

IV. NOMA combined with FBMC and UFMC

NOMA is one of the relevant new RAT proposed for 5G NR. Its objective is to enhance channel capacity by exploiting the power domain. Users can transmit at once with different power levels on the same band. Receivers perform this tricky method to separate signals using the SIC technique as applied in [16], [29].

NOMA can be contextualized in vehicular environment both for DownLink (DL) and UpLink (UL). It superposes signals during transmission, and every single receiver extracts its own signal using SIC. In DL, the gNB performs frequency reuse by superposing two user signals with NOMA. In UL, the receiver performs SIC in order to extract the transmitted bit streams generated using an FBMC modulator as shown in Figure 1(a). Note that the receiver applies SIC without considering the channel estimation and equalization as well as bit error correction. These operations might be included to measure the global impact of our scheme. Two main different NOMA schemes are defined.

Power Domain NOMA (PD-NOMA): the users can use the same channel simultaneously by applying power domain multiplexing at the transmitter and SIC at the receiver. SIC phase is done to decode signals sensed at different power levels and might suffer from co-channel interference. Spectrum efficiency is enhanced like for OMA [16].

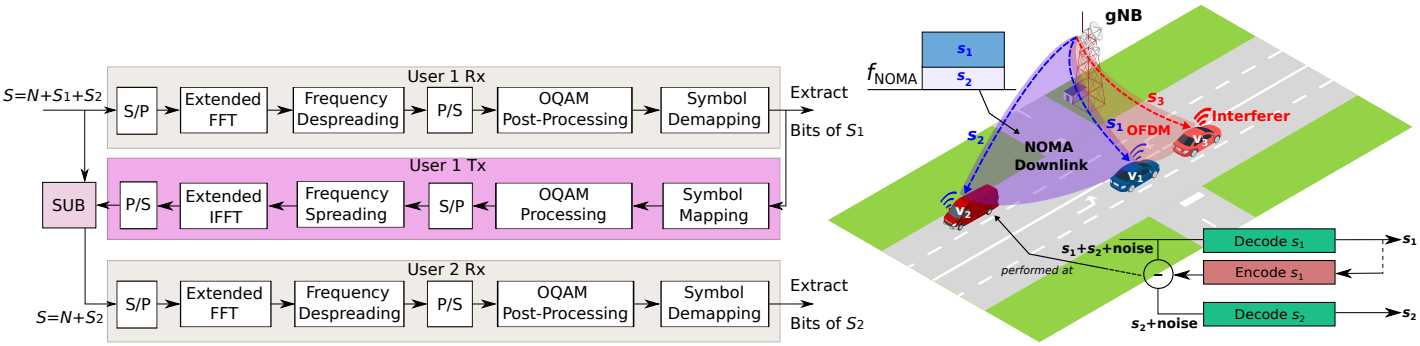

Fig. 1. Successive Interference Cancellation using an FBMC modulator ((a), left); NOMA DL in vehicular environment with OFDM interferer ((b), right).

Code Domain NOMA (CD-NOMA): or Sparse Code Multi-Access (SCMA). It uses sparse spreading sequences: each user bit stream is mapped to different codewords and multiplexed over the dedicated subchannel [30].

In order to apply the SIC technique, the involved users have to be distinguished: i) the Cell Center User (CCU) is the closest user to the gNB, and a Cell Edge User (CEU) is a user located at the cell coverage border. The ideal SIC receiver is the CCU. It should be perfectly able to cancel CEUs embedded signals considered as Gaussian noise by decoding the received main CCU signal at the highest power. In reality, the following two types of SIC receivers are considered:

Symbol-level SIC receiver: at which hard decision without channel decoding is performed on the demodulated signal of the cell edge user. Once obtained, SIC is then applied to remove interference from it by improving the Signal Interference Noise Ratio (SINR) [31].

Codeword-level SIC receiver: at which the same first signal is demodulated and decoded. The channel decoding represents the main difference from the previous case. This improves performances and accuracy in signal recovery, but complexity and latency increase. Optimal performances are reached with receivers with high probability of signal correct recovery and low latency and complexity [31].

As exploited in the next section dedicated for simulation, we consider a use case of DL transmissions issued from a gNB to two V-UEs v_1 and v_2 using NOMA. v_1 (the CCU) is able to directly perform decoding because it receives the highest power signal s_1. v_2 (a CEU) has instead to do successive cancellations before extracting the signal s_2 (see Figure 1 (b)). As mentioned earlier, NOMA allows a significant increase of spectral efficiency since the bandwidth of channel f_{NOMA} is simultaneously used by both V-UEs. The third signal s_3 sent to v_3 (the interferer) is OFDM-modulated on a second channel adjacent to f_{NOMA}. More details about the role of v_3 in the scenario are provided at the end of the next section.

V. Simulation Results

NR-V2X performances in urban vehicular environments are naturally submitted to the fading phenomenon, typically modeled by statistical models representing the Power Delay Profile (PDP). The power reaching a V-UE by DL propagated signals is distributed according to those models, and they involve two main components Line-Of-Sight (LOS) and Non-LOS (NLOS) since the gNB might or not have a direct communication path reaching the V-UE.

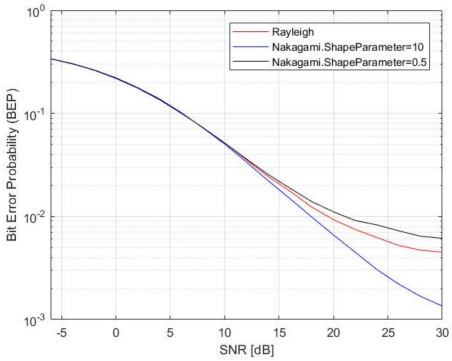

Fig. 2. Rayleigh vs. Nakagami BEPs for OFDM with QPSK applied. The channel model includes Additive White Gaussian Noise (AWGN) and all the Resource Elements composing a RB are modulated with the same symbol constellation.

Rayleigh [32] and Nakagami [33] are two of the most used models. They mainly differ on the dominance/impotence of the LOS component. Their Probability Density Functions (PDFs) are defined as follows.

$$\text{Rayleigh PDF: } \frac{r}{\sigma^2} e^{-\frac{r^2}{2\sigma^2}} \text{ for } r \geq 0 \tag{1}$$

$$\text{Nakagami PDF: } \frac{2}{\Gamma(m)} \left(\frac{m}{w}\right)^m r^{2m-1} e^{-\frac{m}{w} r^2} \text{ for } r > 0 \tag{2}$$

where the random variable r is the envelope amplitude of the received signal, $2\sigma^2$ is the pre-detected mean power of the multipath signal, $\Gamma(\cdot)$ is the Gamma function, and $m \geq 1/2$ (resp. $w > 0$) is the Nakagami shape (resp. spread) parameter.

Model (1) is most applicable when there is no dominant propagation along the LOS component. Model (2) depends on m and w to determine dominance/impotence of the LOS component. By fixing $w = 2\sigma^2$ and varying m, several cases are obtained: i) Nakagami and Rayleigh are equivalent when $m = 1$; ii) worse fading compared to Rayleigh when $m < 1$; iii) presence of the LOS component when $m > 1$. Notice that only the LOS component remains when $m \to \infty$.

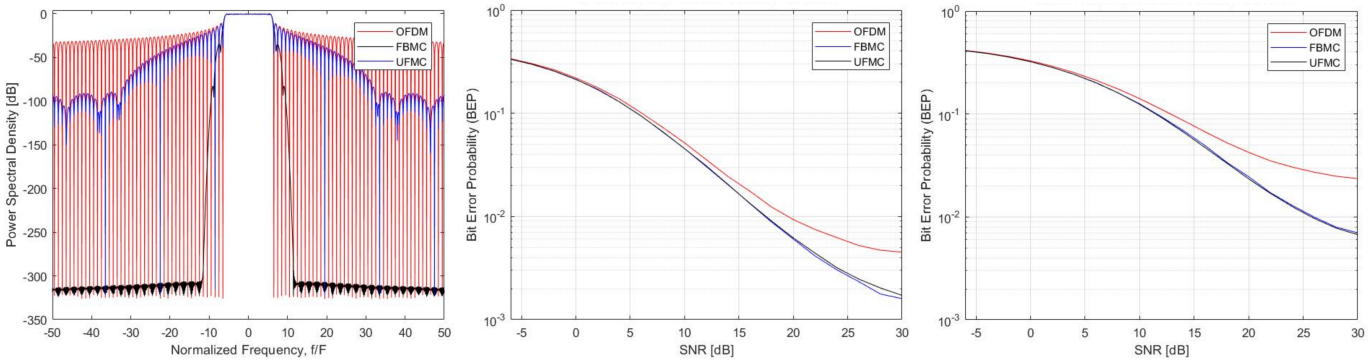

Fig. 3. PSDs of OFDM, FBMC and UFMC ((a), left); Rayleigh's BEPs with QPSK ((b), middle) and 16-QAM ((c),right) modulations.

Figure 2 depicts different settings of the shape parameter m of the Nakagami PDF (0, 0.5 and 10) generating different BEP curves for OFDM with QPSK applied. They perfectly fit theory: the higher the value of m, the better the performances are (LOS component becomes stronger *i.e.,* fading is lower).

TABLE I
SIMULATION PARAMETERS

Fading model	Rayleigh (no dominant LOS propagation)
Subcarrier spacing	15KHz
Number of subcarriers	12
Number of symbols	14
Central frequency	3.6GHz (5G frequency band)
Reflected paths	200
Velocity	80Km/h
Modulation schemes	OFDM, FBMC, UFMC
Symbols constellations	QPSK, 16-QAM

Our simulations were performed using MATLAB (source code is publicly available in GitHub[1] for reproduction and further development). Table I shows the parameters (according to LTE-V) used for the simulation of doubly-selective channels in vehicular environments. We recall that each RB is formed by 12 subcarriers and 7 symbols. Since the subcarrier spacing is 15KHz large, the bandwidth is $15\times12=180$KHz large. The modulation schemes produce three different Power Spectrum Densities (PSDs) for OFDM, FBMC and UFMC as shown in Figure 3(a). They clearly highlight the different natures of the waveforms. In particular, the OBB emissions are clearly reduced under FBMC and UFMC compared to OFDM. Indeed, the OFDM spectrum does not have high side lobes attenuation, leading to substantial interference between adjacent channels. We confirmed that UFMC has low OOB radiation but not as low compared to FBMC. The impact on communication would be significant in terms of low BEP.

Figures 3(b) and 3(c) show the obtained BEPs in terms of Signal-to-Noise Ratio (SNR) variation by changing constellation cardinality (QPSK and 16-QAM) for the three considered waveforms. The simulation was performed by applying the Monte Carlo method, repeating several times the experiment, and computing the average BEPs. As expected, the best curve is that of QPSK since its constellation cardinality is lower than that of 16-QAM riding up more approximated error probability, as expressed in equation (3).

$$P(e) \approx \frac{1}{2}\mathrm{erfc}\left(\sqrt{\frac{d_{\min}^2}{Eb}\frac{Eb}{N0}}\right) \tag{3}$$

The complementary error function is defined by erfc, and the term $Eb/N0$ is proportional to the SNR. Since $\mathrm{erfc}(\cdot)$ is decreasing, if the normalized minimum distance $d_{\min}^2/Eb$ decreases by increasing the constellation cardinality, the error probability increases. By analyzing the difference between the waveform curves for a given constellation, the worse behavior of OFDM compared to the others is due to its higher sensitivity to the channel variations.

By analyzing Figures 3(b) and 3(c), we notice that FBMC and UFMC curves (almost similar with a slight advantage for FBMC over UFMC) give better BEP results than OFDM. They show more resistance to doubly-selective channels and favor requirements of V2X safety (non-safety) applications to be met. The idea is therefore to exploit FBMC to alleviate the interference and to increase the channel capacity in order to support higher data rates.

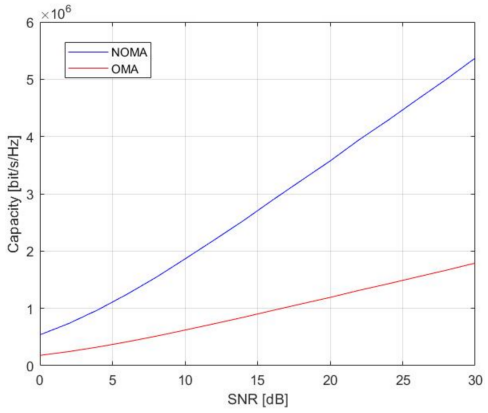

Fig. 4. Channel capacity under NOMA compared to OMA.

These results would be improved by performing multiple access via NOMA by transmitting multiple main carriers over the same time/frequency slot. We consider for that the use case

[1]`https://github.com/zitouni/NOMA-FBMC-UFMC.git`

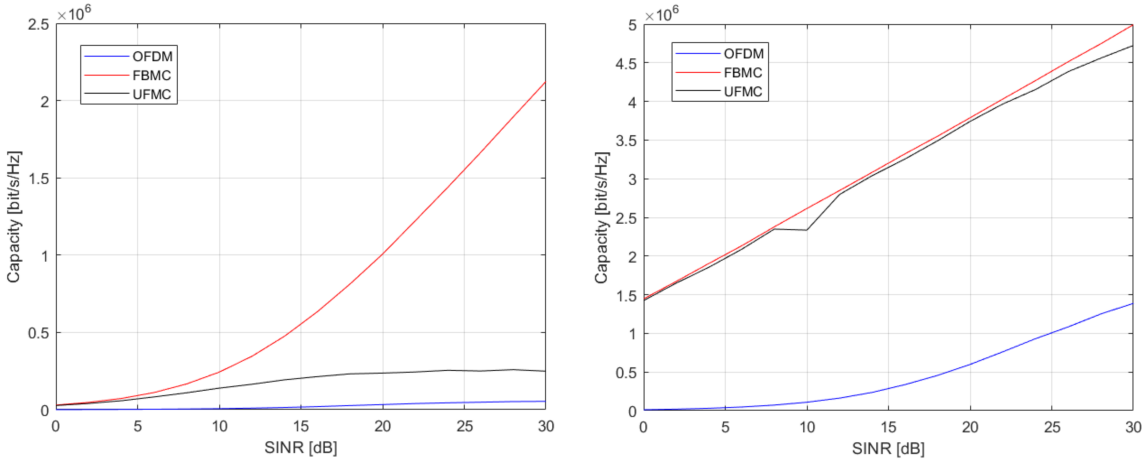

Fig. 5. Channel capacity of OFDM, FBMC and UFMC combined to NOMA scheme in case of high ((a), left) and low ((b), right) OFDM interference.

of Figure 1(b). The gNB exploits the total carrier with PD-NOMA (see Section IV) according to the following equation describing a transmitted signal s:

$$s = \sqrt{p_1}s_1 + \sqrt{p_2}s_2 \tag{4}$$

where s_1 and s_2 are the signals transmitted to v_1 and v_2 resp. with output powers p_1 and p_2. Figure 4 depicts the channel capacities under NOMA and OMA as function of SNR (according to the Shannon formula [34], [35]). The gap between the capacity curve of NOMA compared to that of OMA is clearly significant as expected.

Our study would be limited by a simple case in order to fully demonstrate that NOMA improves the spectrum efficiency face to co-channel interference. According to the scenario shown in Figure 1(b) and considered for simulations, the gNB performs transmission on two adjacent channels. On the first, NOMA is used to communicate with v_1 and v_2. On the second, OFDM is used to communicate with v_3 (the signal s_3). Obviously, the simulation is performed using the same parameters given in Table I to evaluate its spurious emissions (see Figure 3(a)). In mobile/vehicular environments, several users try to access simultaneously the resources. High/low interference may happen between adjacent channels depending on the power domain multiplexing. We distinguish two cases where the interferer is at the highest/lowest output power compared to that of the other users. The scalability is implicitly handled by the simulations since high interference on the adjacent channel might be caused by an important number of interferers. In the first case, the transmission output power of the interferer is 12dB higher than the NOMA user *e.g.,* the "high interference case". The interferer output power is 12dB lower than that of the NOMA user in the second *e.g.,* the "low interference case". As the 5G technology recommends the usage of beamforming making the communication more directional between the gNB and the V-UEs, thus, we kept the number of V-UEs involved in a DownLink communication limited to two.

Simulation results of the channel capacity are obtained in terms of SINR variations according to the following Shannon formula:

$$C_{v_{\text{NOMA}}} = B\log_2(1 + \frac{P_{\text{tx}}}{P_{\text{nz}} + P_{\text{int}}}) \tag{5}$$

where B is 3dB bandwidth of the considered waveform, P_{tx} is the transmission power, P_{nz} is the noise power, and P_{int} is the interference power. Figure 5(b) clearly shows that FBMC channel capacity outperforms the others (UFMC allows a slightly better capacity than OFDM). This is explained by the rectangular shape of FBMC waveform which is characterized by very low lateral lobes (as shown in Figure 3(a)).

UFMC recognizes a better behavior than OFDM in terms of spurious emissions but its power spectrum does not drastically decrease to zero (as shown in Figure 3(a)), and this becomes significant under high interference. It should be noted that channel capacity is highly different between the three curves since high interference decreases the logarithm term of the capacity formula 5. The results are visibly significant since the maximum capacity value obtained for FBMC is 8 times higher than its maximum value under UFMC and 9 times higher than that under OFDM.

In the low interference case, the interferer transmits at lower power with the highest power level assigned to NOMA users: this causes a significant increase of the channel capacity up to 5 (bits/s)/Hz. By analyzing Figure 5(b), the FBMC curve is always the best but its performance is almost similar to that of UFMC, and this can be explained by focusing on SINR effects: the UFMC spurious emissions have quite the same impact as FBMC ones. When the SNR is equal to 10 dB the obtained channel capacity drops suddenly with UFMC. This loss of capacity about 0.5 bit/s/Hz is negligible compared to the significant difference between UFMC and OFDM. OFDM remains at significant low performances due to its OOB emissions even with low interferer power. In this case, FBMC maximizes the channel capacity at least 3.5 times higher than that of OFDM, but keeps it only 5% higher compared to that of UFMC.

VI. Conclusions

The approach of combining FBMC and UFMC with NOMA for V2X communications, presented in this paper, has been analyzed in terms of BEP and channel capacity. According to the simulation results, we found that our approach is relevant not only to improve the channel capacity but also to reduce co-channel interference of V2X communications. We observed that BEP performances vary over the SNR combined with low OOB emissions in the frequency domain as well. Furthermore, NOMA increases the channel capacity compared to OMA even in the presence of adjacent channel interference. And when combined with FBMC, the capacity is improved at least by 3.5 times. Meanwhile, the main issues are scalability and channel estimation and equalization. On the one hand, the estimation and equalization shall be performed to achieve a correct SIC. On the other hand, scalability is required at transmission since each connected system shall adjust its own output power and keep it different compared to others while they are with a limited power domain.

Acknowledgement

We would like to thank Mattia Minelli for his insights into NOMA and FBMC radio access technologies.

References

[1] C. Sommer and F. Dressler, *Vehicular Networking*. Cambridge University Press, 2014.

[2] IEEE Standards Association, "802.11-2016 - IEEE Standard for Information technology—Telecommunications and information exchange between systems Local and metropolitan area networks—Specific requirements - Part 11: Wireless LAN Medium Access Control (MAC) and Physical Layer (PHY) Spec," IEEE, Std., 2020.

[3] Third Generation Partnership Project, "Release 14 Description; Summary of Rel-14 Work Items," UIT, ETSI, CCSA, ATIS, TTA, Std., 2018.

[4] W.-D. Shen and H.-Y. Wei, "Distributed V2X Sidelink Communications With Receiver Grant MAC Design," *IEEE Trans. on Vehicular Technology*, vol. 71, no. 5, pp. 5415–5429, 2022.

[5] IEEE P802.11-Task Group BD, "Status of Project IEEE P802.11bd," 2018, https://www.ieee802.org/11/Reports/tgbd_update.htm.

[6] M. H. C. Garcia, A. Molina-Galan, M. Boban, J. Gozalvez, B. Coll-Perales, T. Şahin, and A. Kousaridas, "A tutorial on 5G NR V2X communications," *IEEE Com. Surveys & Tutorials*, vol. 23, no. 3, pp. 1972–2026, 2021.

[7] M. Harounabadi, D. M. Soleymani, S. Bhadauria, M. Leyh, and E. Roth-Mandutz, "V2X in 3GPP Standardization: NR Sidelink in Release-16 and Beyond," *IEEE Com. Standards M.*, vol. 5, no. 1, pp. 12–21, 2021.

[8] S. Chen, J. Hu, Y. Shi, Y. Peng, J. Fang, R. Zhao, and L. Zhao, "Vehicle-to-Everything (V2X) Services Supported by LTE-Based Systems and 5G," *IEEE Com. Standards M.*, vol. 1, no. 2, pp. 70–76, 2017.

[9] Third Generation Partnership Project, "LTE-Advanced (3GPP Release 10 and beyond)," UIT, ETSI, CCSA, ATIS, TTA, Std., 2009.

[10] B. Farhang-Boroujeny, "OFDM Versus Filter Bank Multicarrier," *IEEE Signal Processing M.*, vol. 28, no. 3, pp. 92–112, 2011.

[11] R. Nissel and M. Rupp, "OFDM and FBMC-OQAM in Doubly-Selective Channels: Calculating the Bit Error Probability," *IEEE Com. Let.*, vol. 21, no. 6, pp. 1297–1300, 2017.

[12] V. Vakilian, T. Wild, F. Schaich, S. ten Brink, and J.-F. Frigon, "Universal-filtered multi-carrier technique for wireless systems beyond LTE," in *IEEE Global Com. Conf. (GC'13) Works.*, 2013, pp. 223–228.

[13] K. Zerhouni, R. Elassali, F. Elbahhar, K. Elbaamrani, and N. Idboufker, "On the cyclostationarity of Universal Filtered Multi-Carrier UFMC," *AEU Int. J. of Electronics & Com.*, vol. 89, pp. 174–180, 2018.

[14] X. Zhang, M. Jia, L. Chen, J. Ma, and J. Qiu, "Filtered-OFDM - Enabler for Flexible Waveform in the 5th Generation Cellular Nets." in *IEEE Global Com. Conf. (GC'15)*, 2015, pp. 1–6.

[15] Y. Saito, Y. Kishiyama, A. Benjebbour, T. Nakamura, A. Li, and K. Higuchi, "Non-Orthogonal Multiple Access (NOMA) for Cellular Future Radio Access," in *IEEE Vehicular Technology Conf. (VTC-Spring'13)*, 2013, pp. 1–5.

[16] K. Higuchi and A. Benjebbour, "Non-orthogonal Multiple Access (NOMA) with Successive Interference Cancellation for Future Radio Access," *IEICE Trans. on Com.*, vol. E98.B, pp. 403–414, 2015.

[17] Third Generation Partnership Project, "Release 17 Description; Summary of Rel-17 Work Items," UIT, ETSI, CCSA, ATIS, TTA, Std., 2022.

[18] T. Kebede, Y. Wondie, J. Steinbrunn, H. B. Kassa, and K. T. Kornegay, "Multi-Carrier Waveforms and Multiple Access Strategies in Wireless Nets.: Performance, Applications, and Challenges," *IEEE Access*, vol. 10, pp. 21 120–21 140, 2022.

[19] H. Hesham and T. Ismail, "Hybrid NOMA-based ACO-FBMC/OQAM for next-generation indoor optical wireless communications using LiFi technology," *Optical & Quantum Elecs.*, vol. 54, no. 3, pp. 1–17, 2022.

[20] I. Baig, U. Farooq, N. U. Hasan, M. Zghaibeh, and V. Jeoti, "A Multi-Carrier Waveform Design for 5G and beyond Communication Systems," *Mathematics J.*, vol. 8, no. 9, p. 1466, 2020.

[21] Z. Ding, R. Schober, and H. V. Poor, "Unveiling the Importance of SIC in NOMA Systems—Part 1: State of the Art and Recent Findings," *IEEE Com. Let.*, vol. 24, no. 11, pp. 2373–2377, 2020.

[22] A. Latunde, A. Papazafeiropoulos, P. Kourtessis, and J. Senior, "Co-existence of OFDM and FBMC for Resilient Photonic Millimeter-Wave 5G Mobile Fronthaul," *Photonic Net. Com.*, vol. 37, p. 335–348, 2019.

[23] Y. Qi and M. Al-Imari, "An Enabling Waveform for 5G – QAM-FBMC: Initial Analysis," in *IEEE Conf. on Standards for Com. and Net. (CSCN'16)*, 2016, pp. 1–6.

[24] Third Generation Partnership Project, "Release 16 Description; Summary of Rel-16 Work Items," UIT, ETSI, CCSA, ATIS, TTA, Std., 2020.

[25] M. M. Saad, M. T. R. Khan, S. H. A. Shah, and D. Kim, "Advancements in Vehicular Communication Technologies: C-V2X and NR-V2X Comparison," *IEEE Com. M.*, vol. 59, no. 8, pp. 107–113, 2021.

[26] R. Molina-Masegosa and J. Gozalvez, "LTE-V for Sidelink 5G V2X Vehicular Communications: A New 5G Technology for Short-Range Vehicle-to-Everything Com." *IEEE Vehicular Technology M.*, vol. 12, no. 4, pp. 30–39, 2017.

[27] M. A. Ruder, M. Papaleo, S. Stefanatos, T. V. Nguyen, and S. Patil, "On the Coexistence Between LTE-V2X Sidelink and ITS-G5," in *IEEE Vehicular Net. Conf. (VTC-Spring'21)*, 2021, pp. 162–169.

[28] J. Almeida, M. Alam, J. Ferreira, and A. S. Oliveira, "Mitigating Adjacent Channel Interference in Vehicular Communication Systems," *Digital Com. and Net. J.*, vol. 2, no. 2, pp. 57–64, 2016.

[29] R. Zitouni and S. Tohmé, "Non-Orthogonal Multiple Access for Vehicular Nets. based Software-Defined Radio," in *14th Int. Wireless Com. & Mobile Computing Conf. (IWCMC'18)*, 2018, pp. 1142–1147.

[30] B. Di, L. Song, Y. Li, and Z. Han, "V2X Meets NOMA: Non-Orthogonal Multiple Access for 5G-Enabled Vehicular Nets." *IEEE Wireless Com. M.*, vol. 24, no. 6, pp. 14–21, 2017.

[31] C. Yan, A. Harada, A. Benjebbour, Y. Lan, A. Li, and H. Jiang, "Receiver Design for Downlink Non-Orthogonal Multiple Access (NOMA)," in *IEEE Vehicular Technology Conf. (VTC-Spring'15)*, 2015, pp. 1–6.

[32] B. Sklar, "Rayleigh Fading Channels in Mobile Digital Communication Systems. I. Characterization," *IEEE Com. M.*, vol. 35, no. 9, pp. 136–146, 1997.

[33] M. Nakagami, "The m-distribution–A General Formula of Intensity Distribution of Rapid Fading," in *Statistical Methods in Radio Wave Propagation*. Elsevier, 1960, pp. 3–36.

[34] C. E. Shannon, "A mathematical theory of communication," *The Bell System Technical J.*, vol. 27, no. 3, pp. 379–423, 1948.

[35] C. Shannon, "Communication in the Presence of Noise," *Procs. of the IRE*, vol. 37, no. 1, pp. 10–21, 1949.